Dissolved Cl, Oxygen Fugacity, and Their Effects on Fe Behavior in a Hydrous Rhyodacitic Melt Revision 2

Aaron S. Bell[1,*], James D. Webster[2]

[1]Institute of Meteoritics, University of New Mexico, Albuquerque, NM 87109
[2]Department of Earth and Planetary Science, American Museum of Natural History New York, NY 10024

Abstract

We have conducted a series of experiments to evaluate the intrinsic effects of dissolved chlorine on $Fe^{3+}/\Sigma Fe$ and magnetite solubility in hydrous chloride-rich rhyodaciticliquids. The addition of Cl to the melt appears to have two prominent effects on iron in the melt: 1) Dissolved Cl appears to perturb the magnetite-melt equilibrium, such that greater FeO^{total} contents are required to support magnetite saturation in Cl-bearing melts than in Cl-free melts of equivalent bulk compositions; and 2) a systematic and progressive decrease of the measured $Fe^{3+}/\Sigma Fe$ as fO_2 is increased. These two intimately related effects each have important implications for redox processes occurring in Cl-enriched arc magmas.

Introduction

Iron is by far the most abundant multivalent element present in terrestrial magmas (Wilke 2005) and therefore exerts a proportionally large influence on the overall redox behavior of natural silicate melts. Much analytical and experimental effort has been exerted in order to illuminate the relationships between the molar ratio of $FeO_{1.5}/FeO$ and intensive parameters such as bulk melt composition, pressure, and temperature (Sack et al. 1980; Kilinc et al. 1983; Kress and Carmichael 1991; Tangeman et al., 2001; Ottonello et al. 2001; Jaysauria et al. 2004; Moretti 2005; Borisov and McCammon 2010). Previous efforts have also been extended to account for the effects of dissolved volatile constituents on Fe redox behavior. Specifically, the intrinsic effects of dissolved water on the equilibrium ratio of ferric and ferrous iron have been the subject of several studies as well as the source of much debate and controversy (Moore et al. 1995; Baker and Rutherford 1996; Gaillard et al. 2001; Wilke et al. 2002).

Though a considerable quantity of work has been directed toward understanding dissolved water's effects on the redox systematics of Fe, the potential effects of other volatile elements that fill anionic structural roles have only been investigated to a limited extent. After dissolved hydroxyl, chlorine is the second-most abundant anionic volatile component in evolved, subduction-related silicate magmas (Wallace 2005). Given the propensity for Cl to form ionic bonds with divalent cations in silicate melts (Carroll and Webster 1994; Webster and DeVivo 2002; Zimova and Webb 2006; Filliberto and Trieman 2009; Filliberto et al. 2014; Webb et al. 2014; Webster et al. 2015), it is reasonable to hypothesize that dissolved chlorine may exert a significant influence on redox behavior of iron. Such an effect would have important implications for the stability fields of Fe-bearing minerals in equilibrium with chlorinated melts, as well as understanding the relationship between the measured, formal valence of iron and magmatic fO_2. The latter point is of considerable importance, as the formation of Fe-Cl species in the melt (i.e. the formation of a $FeCl_2$ melt component analogous to the oxide component FeO) requires that the relative concentration of Fe^{2+} in the melt is not exclusively determined by magmatic fO_2, but is rather a function of both fO_2 and the Cl content (i.e. fCl_2) of the melt.

This initial hypothesis is supported by the data and conclusions drawn from a number of previous studies on Cl solubility. The pioneering work of Webster and DeVivo (2002) established a quantitative link between the concentration of divalent cations such as Mg, Fe, and Ca and melt Cl-dissolution capacity. Several studies on the effects of Cl on the viscosity of silicate melts observed that the addition of Cl to some Fe-bearing melts results in an increase in the viscosity of these liquids, suggesting that dissolved Cl bonds with Fe^{2+} in the melt and disrupts its network-modifying structural role (Dingwell and Hess 1998; Zimova and Webb 2006; Webb et al. 2014). Additionally, a recent XANES (X-ray Absorption Near Edge Structure) study conducted by Evans et al. (2008) identified dissolved Cl bonded to divalent cations in the form of Mg-Cl and Ca-Cl species in haplobasaltic glasses. Although the melts of this study did not contain Fe, the authors concluded that divalent Ca and Mg form Cl complexes with a short-range

structure similar to that of crystalline $MgCl_2$ and $CaCl_2$. Given the strong similarities between the ionic radius and field strength of Fe^{2+} and Mg^{2+}, it seems probable that Fe-Cl complexes also exist as species in silicate melts. In this work we present a series of experiments designed to investigate the potential relationship between Fe and Cl in a hydrous rhyodacitic liquid. While this work in no way represents a comprehensive study of the effects of Cl on Fe in melts, the experiments presented do provide some new and unique insight into potential Fe-Cl interactions in felsic melts.

Experimental Design and Rationale

Two sets of experiments were conducted, each with a different purpose.

The first set of experiments was designed to investigate the effect of dissolved Cl on magnetite solubility in hydrous chlorinated rhyodacitic melts at controlled fO_2. Iron was added to the starting charges as a single chip of magnetite or a mixture of glass and magnetite powder that was located at one end of the capsule. These experiments were purposefully configured in this manner, so that the melt from only one end of the experimental charge would be in direct contact with magnetite. This set of experiments will be referred to as the MagLiq series.

A second set of melt-only experiments was designed to examine the potential effects of dissolved Cl on the $Fe^{3+}/\sum Fe$ of the quenched rhyodacitic melts over a range of fO_2 values. These experiments have been designated the SRD series. In addition to the Cl-bearing experiments, a few redox-controlled experiments were performed in order to develop additional dacitic-glass XANES standards. Experimental conditions, Fe and Cl concentrations, and the XANES measured $Fe^{3+}/\Sigma Fe$ values for the quenched melts are presented in Table 1.

All of the SRD and MagLiq experiments were performed in 3 mm (OD) × 2.7 mm (ID) × 20 mm (length) Au capsules. At the temperatures of the experiments in this study, Au capsules are sufficiently H_2 permeable to attain redox equilibrium within the first several hours of the experiment (Gaillard et al. 2001). Water and Cl were added to the charges in the form of a Na-K-H chloride solution. Appropriate

quantities (10-15 mg) of a prepared NaCl-KCl-HCl solution (ΣCl = 7.5 wt. %) were added to each SRD2 capsule with a micro-pipette to ensure that each charge remained fluid-saturated throughout the duration of the experiment (each experiment contained from 30-45 mg SRD2 starting glass). The fluid-melt ratios for these experiments are somewhat variable, therefore the extent of Fe scavenging and alkali exchange have differently affected the melt composition of each experiment, albeit to a relatively limited extent. For the MagLiq runs, special care was taken to minimize the fluid-melt ratio present at run conditions in order to mitigate Fe loss and alkali exchange due to fluid scavenging (Bell and Simon 2011).

Experiments were conducted in a Shaw membrane-equipped internally-heated pressure vessel apparatus at the American Museum of Natural History (AMNH). All experimental runs were conducted at 950°C and pressures of either 130 MPa or 150 MPa. Run durations for the equilibrium MagLiq and SRD experiments ranged from 132 to 212 hours. Temperature and thermal gradients were measured with two factory-calibrated, Inconel-sheathed type-K thermocouples. The maximum measured thermal gradient (ΔT) over the length of an experimental capsule was ±7° C. Pressure was measured with a bourdon tube-type strain gauge with a precision of ± 10 bar. Experiments were isobarically quenched at approximately 10 °C sec^{-1}.

The oxidation state of the experimental charges was controlled with a platinum-sheathed Shaw membrane that was positioned immediately adjacent to the experimental capsules. The partial pressure of H_2 transmitted from the membrane to the Ar pressure medium in the vessel was monitored with a high-precision bourdon tube gauge. Oxygen fugacities imposed by the membrane were verified with a solid-state Co-Pd-CoO redox sensor identical to those described by Taylor et al. (1991). Oxygen fugacity calculated from the redox sensor alloy composition ($Co_{39.5}Pd_{40.5}$) was $\log_{10} fO_2$ = -11.75 ± 0.10, in excellent agreement with the anticipated fO_2 of the sensor runs, and therefore all reported pH_2 and fO_2 values are believed to be comparably accurate. The oxygen fugacity of each experimental charge was

calculated using the fH_2 imposed by the Shaw membrane, the fH_2O of the experimental charge, and H_2O formation constant from Robie and Hemmingway (1995).

EPMA and XANES Analytical Details

The EPMA-determined compositions of the equilibrium MagLiq glasses and the glasses from the magnetite-free SRD2 runs are given in Electronic Appendix I. This appendix also contains detailed discussion of the EPMA and XANES analytical procedures, standards, and new XANES standard development.

Results and Discussion

Using Magnetite-Dissolution Experiments to Examine Potential Fe-Cl Interactions in the Melt

Perhaps the most direct way to observe potential Fe-Cl interactions in the melt is by examining the total Fe content (where total Fe content is equal to the sum of all Fe species present in the melt, i.e. Fe-O species and Fe-Cl species) of melts with various Cl contents in equilibrium with magnetite. Many of the MagLiq series experiments did not attain a homogenous Fe distribution in the melt; therefore these experiments were considered to be failed and will not be discussed in this section. The melts in four of the MagLiq series experiments appear to have achieved a uniform Fe distribution, and thus are believed to have attained a steady state. The results from only these experiments will be discussed in this section. The run conditions and the EMP determined Fe and Cl concentrations of the equilibrium MagLiq melts are presented in Table 1.

With these MagLiq series experiments we have attempted to isolate the effects of dissolved chlorine on the Fe^{total} content of the liquid required to support magnetite saturation. The equilibria governing magnetite dissolution illustrate how Cl may affect the EPMA measured iron content (which is reported with the EPMA data as "FeO") of the magnetite saturated melt. The magnetite dissolution reaction may be written as:

$$Fe_3O_4^{mag} = FeO^{melt} + 2FeO_{1.5}^{melt}$$

or alternatively expressed as a simple solubility product:

$$K_1 = (a\mathrm{FeO}^{\mathrm{melt}}) \cdot (a\mathrm{FeO}_{1.5}{}^{\mathrm{melt}})^2$$

Additionally, fixing the $f\mathrm{O}_2$ fixes the ratio of aFeO to $a\mathrm{FeO}_{1.5}$ in melt via the homogenous redox reaction

$$\mathrm{FeO} + 0.25\mathrm{O}_2 = \mathrm{FeO}_{1.5}$$

$$K_2 * (f\mathrm{O}_2)^{-0.25} = a\mathrm{FeO}/a\mathrm{FeO}_{1.5}$$

From these reactions it is clear that perturbation of either aFeO or $a\mathrm{FeO}_{1.5}$ due to changing $f\mathrm{O}_2$ in the melt must be accompanied by either the dissolution or precipitation of magnetite to maintain equilibrium. However at fixed P, T, and $f\mathrm{O}_2$, the only way to perturb the total iron concentration in the melt is by altering the activity coefficients for either FeO or $\mathrm{FeO}_{1.5}$ in the melt. The addition of Cl to the melt appears to produce this result. The results of the MagLiq experiments unequivocally show that the addition of Cl to the melt is accompanied by a significant increase in the EPMA-determined total iron content of the quenched melt (see Table 1). For example, experiments MagLiq5 (Cl-bearing) and MagLiq6 (Cl-free) have EPMA-determined total Fe contents of 4.9 ± 0.16 wt % and 4.2 ± 0.21 wt %, respectively (these values are reported as FeO in Table 1). The magnitude of the increase in Fe is not large, yet it is shown to be highly statistically significant when evaluated with a Student's T-test (the calculated two-tailed P-value for MagLiq 5 and 6 is <0.0001).

The observed increase in the iron concentration of the Cl-bearing experiments requires the presence of dissolved Cl to depress aFeO or $a\mathrm{FeO}_{1.5}$ in the melt. Given what is known about potential Cl speciation in melts, there are two possible explanations for this behavior. The simplest explanation is that anionic Cl bonds with Fe in the melt to form stable Fe-Cl complexes, therefore lowering the activities of the Fe-O species in the melt. The second explanation requires the formation of Mg^{2+}-Cl, Ca^{2+}-Cl, or Na^{1+}-Cl in the melt; the presence of these complexes in some way fundamentally and indirectly changes aFeO and $a\mathrm{FeO}_{1.5}$. It is important to note that the mechanisms presented above are not mutually exclusive, and that dissolved Cl is likely distributed among many competing divalent and

monovalent cations. Unfortunately the magnetite dissolution experiments cannot be used to rigorously test the "direct Fe-Cl speciation" hypothesis versus the "indirect complexing effect" hypothesis. The experiments described in the next two sections supplement the observations from the MagLiq experiments, further clarifying the chemical links between Fe and Cl in the melt.

Evidence for Fe-Cl Interaction from a Failed, Disequilibrium Magnetite Dissolution Experiment

As discussed in the previous section, many of the magnetite-dissolution experiments failed to attain a uniform iron distribution in the melt. Although the failed experiments do not accurately depict the equilibrium iron content of the melt, they do capture a unique kinetic aspect of the magnetite-dissolution process that illuminates the chemical link between Fe and Cl in the melt. This section presents EPMA data from an analytical transect taken from the run products of one of the "failed" experiments. Figure 1a is a composite BSE (backscattered electron) image of the condensed products of one of the "disequilibrium" magnetite-dissolution experiments. Superimposed on this BSE image is the location of an EMP analytical transect across the quenched liquid. The compositional data plotted in Figure 1b show a thought-provoking relationship between the concentration profiles for FeO^{total} and Cl. As expected, the FeO^{total} content of the liquid monotonically decreases with distance from the interface of the magnetite-bearing and magnetite-free portions of the melt. The FeO^{total} content of the liquid nearest to the magnetite bearing melt appears to be a uniform ~5.5 wt% before decreasing to approximately 3.5 wt % in the distal portion of the glass.

We have interpreted this FeO^{total} distribution as a diffusion profile. In contrast to Fe, Cl appears to increase as the magnetite-melt interface is approached. The apparent redistribution of what was in the initial hours of the experiment a homogenous Cl concentration suggests that a Cl speciation reaction co-occurring with magnetite dissolution is causing this behavior. An example of such a speciation reaction involving Fe-Cl species is:

$$CaCl_2^{melt} + FeO^{melt} = FeCl_2^{melt} + CaO^{melt}$$

The addition of Fe to the melt from the magnetite dissolution results in the formation of Fe-Cl species. The Fe-enrichment of the melt causes in the stabilization of Fe-Cl species results in a melt with higher Cl solubility. It is the enhanced Cl solubility that is responsible for inducing a temporary Cl chemical potential in the melt. The existence of this gradient causes the observed "uphill" diffusive flux of Cl. If no interactions between melt components were occurring, the Cl content of the melt would simply decrease by dilution in the region adjacent to the magnetite-melt interface. Similar dissolution-diffusion arguments for melt speciation reactions have been invoked to describe homogenous alkali-Al speciation reactions in hydrous, haplogranitic melts (Acosta-Vigil et al. 2002, 2006). Using reasoning analogous to that presented in those studies, we conclude that the observed correlation between Fe and Cl concentrations suggests the occurrence of a Fe-Cl speciation reaction in the melt. The speciation reaction presented above should not be interpreted to mean that no other Cl species exist in the melt, but rather that Cl is distributed among the available cations in the melt in a manner that reflects the hierarchy of their relative stabilities. It is important to note that the results of the dis-equilibrium dissolution experiments cannot indicate which form of iron oxidation state -ferric or ferrous- is primarily involved in the proposed Cl-complexing reactions.

A Causal Link between Fe-Cl Speciation and the Relationship between $Fe^{3+}/\Sigma Fe$ and fO_2?

In this section we focus primarily on the relationship between fO_2 and the response of the measured Fe valence in the melt. It is important to point out that XANES measurements themselves can only yield information about the formal valence state of iron in the melt; therefore, the XANES-measured $Fe^{3+}/\Sigma Fe$ values of the glasses for the SRD experiments are given in Table 1 and have been plotted in Figure 2. The measured $Fe^{3+}/\Sigma Fe$ ranges from a low of 0.28 a high of 0.42. This relatively restricted range of values is remarkable, considering that the fO_2 varied in excess of three orders of magnitude in these experiments. The $Fe^{3+}/\Sigma Fe$ only increases by approximately 13%, as the experimentally imposed fO_2 increases from FMQ to FMQ + 3.2. To place this observation in context, the Kress and Carmichael (1991) model

197 indicates that $Fe^{3+}/\Sigma Fe$ for the SRD melt should increase at nearly twice this rate in response to a 3.2 log
198 unit increase in fO_2. The relationship between $Fe^{3+}/\Sigma Fe$ and fO_2 that we have observed for the
199 chlorinated SRD melts is unique. No previous studies have yielded similar results with respect to the
200 *slope* of the ferric-ferrous ratio as a function of fO_2. In all previous studies of hydrous melts, none of
201 which contained Cl, the observed relationship between $Fe^{3+}/\Sigma Fe$ and fO_2 has been consistent with the
202 apparent reaction stoichiometry as either defined by the Kress and Carmichael (1991) equation, or the
203 theoretical reaction stoichiometry (Jayasauria et al. 2004). The Fe valence data from the SRD
204 experiments suggest that the addition of Cl to the melt fundamentally changes the relationship between
205 Fe valence and fO_2, as the rate at which the measured Fe^{3+} abundance increases in the melt appears to
206 be damped.

207 The relationship between $Fe^{3+}/\Sigma Fe$ and fO_2 observed in the SRD experiments may be interpreted in a
208 number of different ways. Here we present two possible interpretations of the Fe^{3+}/Fe data: (1) the
209 formation of Fe^{2+}-Cl species partially decouples the measured formal valence ratio from the imposed
210 experimental fO_2, and (2) the changes in Cl-speciation in the melt co-occurring with Fe oxidation alter
211 the activity ratio of FeO and $FeO_{1.5}$ in the melt. It is important to note that these interpretations are not
212 mutually exclusive, and that the mechanisms proposed may both significantly affect the equilibrium
213 $Fe^{3+}/\Sigma Fe$.

214 In the first interpretation, the addition of Cl to the melt results in the formation of Fe^{2+}-Cl species. If
215 such a species exists in the melt, then the denominator of the $Fe^{3+}/\Sigma Fe$ ratio is partially controlled by the
216 abundance of the Fe^{2+}-Cl species in the melt. As fO_2 in the melt is increased, the $FeO_{1.5}/FeO$ ratio may
217 indeed still increase following the expected stoichiometry, however, the persistent presence of Fe^{2+}-Cl
218 species in the higher fO_2 experiments acts to suppress the expected increase in the measured $Fe^{3+}/\Sigma Fe$
219 with fO_2. Realistically, this simplified explanation may be complicated by homogenous Cl speciation

reactions, as the abundance of FeCl species may be, in part, linked to the activity of FeO in a complex way.

It is also possible to rationalize the observed Fe^{3+}/Fe^{2+} versus fO_2 trend by considering how the distribution of Cl species in the melt changes as a function of fO_2. The preponderance of the available Cl solubility and phase equilibrium studies suggest that many different cations are ultimately involved in forming Cl species within the melt. Therefore it follows that the Cl content of the melt is not simply determined by a single canonical Cl species, but rather it is a reflection of a hierarchical distribution, where Cl is appropriated among the various competing cations according to the relative stabilities of their Cl complexes. The results of Webster and DeVivo (2002) indicate that the relative stability of Cl species follows a general pattern where Ca^{2+}-Cl = Mg^{2+}-Cl > Fe^{2+}-Cl >> Na^{1+}-Cl > K^{1+}-Cl. As such the distribution of Cl species in the melt can be described as a series of homogenous speciation reactions:

$$FeCl_2 + Na_2O = FeO + 2NaCl$$

$$FeCl_2 + CaO = FeO + CaCl_2$$

$$FeCl_2 + K_2O = FeO + 2KCl$$

At fixed melt composition, temperature, pressure, and fO_2, the distribution of Cl species is fully defined by a combination of the appropriate homogenous speciation equilibria. It therefore follows that under more oxidized conditions the apparent speciation behavior of Cl should change substantially. In the case of our experiments, it appears that increasing fO_2 disturbs the equilibrium distribution of Cl in the melt by decreasing the availability of Fe^{2+} to form $FeCl_2$ species. If the Cl concentration of the melt remains nearly constant, as it does in our experiments, then the decreased FeO content of the melt must be accompanied by a concomitant shift in the Cl species distribution. Increasing fO_2 effectively redistributes some Cl that was formerly bonded to Fe^{2+} to form Cl complexes with the alkalis and alkaline earth cations. In other words, at higher fO_2, the Cl speciation shifts to favor the formation of Na-Cl or Ca-Cl

243 species over Fe^{2+}-Cl species. The result of this process is an effective depression of the Na_2O/NaCl,
244 K_2O/KCl and CaO/$CaCl_2$ ratios in the melt.

245 Redox-induced changes in Cl speciation may also be responsible for suppressing the formation of
246 $FeO_{1.5}$ with increasing experimental fO_2. Increased abundances of $CaCl_2$, NaCl, and KCl in the melt appear
247 to decrease the "effective" alkalinity of the melt, thus depressing the equilibrium Fe^{3+}/ΣFe. The
248 relationship between melt alkalinity and Fe^{3+}/ΣFe has been well documented by numerous studies
249 (Mysen et al. 1980; Sack et al. 1980; Kress and Carmichael 1991). These studies have unanimously
250 shown that increasing concentrations of K_2O, Na_2O, and CaO cause an increase in the equilibrium
251 Fe^{3+}/ΣFe at constant fO_2. This effect has been attributed to the structural role of these cations as
252 possible charge compensators for $^{IV}Fe^{3+}$ in the melt by forming species such as $NaFe^{3+}O_2$ (Mysen et al.
253 1980). Our data suggest chlorinated alkalis may not effectively act as charge compensators for $^{IV}Fe^{3+}$ in
254 bonding configurations such as Fe^{3+}-Cl-Na^{1+}. Alternatively, the effects of changing Cl-speciation on the
255 melt alkalinity may be understood in terms of the link between polymerization state and optical basicity
256 of a melt and its equilibrium Fe^{3+}/ΣFe (Ottonello et al. 2001). In the case of our experiments, formation
257 of alkali- and alkaline earth-Cl complexes may decrease the NBO/T (non-bridging oxygen per tetrahedral
258 cation) and basicity of the melt, thereby enhancing the stability of $Fe^{2+}O$ species in the melt. The effects
259 of Cl on the NBO/T of natural aluminosilicate melts may in fact be significantly more complex than the
260 simple relationships described above, therefore the potential importance of the role of Cl in altering the
261 Fe^{3+}/ΣFe via changing the melt NBO/T is still an open question.

262 **Implications for Ore-Forming Processes and Cl-Rich Arc Magmas:**

263 It has been proposed that onset of magnetite crystallization plays a critical role in modulating the
264 onset of Fe-Cu sulfide saturation in arc magmas (Jenner et al. 2010). In this way, the suppressing effect
265 of Cl on magnetite saturation may help keep the sulfide in Cl-enriched arc magmas under-saturated until
266 an exsolved volatile phase has removed a significant quantity of Cl from the melt. From the perspective

of ore deposit formation, the timing of sulfide saturation controls the total metal budget of the causative magma; it is therefore critical that the role of Cl is understood in the context of how it alters the stability of ferric iron bearing minerals.

Additionally, the equilibrium $Fe^{3+}/\Sigma Fe$ of the melt is significantly affected by the presence of Cl. This relationship may be the effect of two different but complimentary mechanisms - the formation of ferrous-chloride complexes in the melt as well as the formation of alkali chloride species. In either case, the removal of Cl from the melt will result in the stabilization of $FeO_{1.5}$ at the expense of FeO, provided that the system is open with respect to oxygen (or H_2, as the case may be). Though this initial work hints at the important relationship between Fe and Cl in felsic-intermediate melts, much more work is required to fully appreciate and understand the extent to which Cl may alter the fundamental redox behavior and phase equilibria of arc magmas.

Acknowledgements

ASB thanks the AMNH for providing the Kalbfleisch Postdoctoral Fellowship and additional funding, without which this work would not have been possible. We thank M. Newville at APS for his assistance with the acquisition of the XANES spectra and the subsequent data processing, M. D. Dyar and E. Breves are thanked for their assistance in the acquisition and interpretation of the Mössbauer data. We are also indebted to D. Ebel and M. Wilke for providing valuable discussion and informal reviews of an early version of this manuscript. E. Cottrell is thanked for graciously providing the set of rhyolitic glass standards. Portions of this work were performed at GeoSoilEnviroCARS (Sector 13), Advanced Photon Source (APS), Argonne National Laboratory. GeoSoilEnviroCARS is supported by the National Science Foundation - Earth Sciences (EAR-1128799) and Department of Energy - Geosciences (DE-447 FG02-94ER14466). Use of the Advanced Photon Source was supported by the U. S. Department of Energy, Office of Science, 448 Office of Basic Energy Sciences, under Contract No. DE-AC02-06CH113.

References

Acosta-Vigil, A., London, D., Dewers, T., and Morgan, G.B. (2002) Dissolution of corundum and andalusite in H_2O-saturated haplogranitic melts at 800°C and 200 MPa: constraints on diffusivities and the generation of peraluminous melts Journal of Petrology, 43, 1885–1908.

Acosta-Vigil, A., London, D., Dewers, T., and Morgan, G.B. (2006) Dissolution of quartz, albite, and orthoclase in H_2O-saturated haplogranitic melt at 800 °C and 200 MPa: diffusive transport properties of granitic melts at crustal anatectic conditions Journal of Petrology, 47, 231 254.

Baker, L.L., Rutherford, M.J. (1996) The effect of dissolved water on the oxidation state of silicic melts. Geochimica et Cosmochimica Acta 60, 2179–2187.

Bell, A.S., and Simon, A. (2011) Experimental evidence for the alternation of $Fe^{3+}/\sum Fe$ of silicate melt caused by chlorine rich aqueous volatiles. Geology

Borisov, A., and McCammon, C. (2010) The effect of silica on ferric/ferrous ratios in silicate melts: An Experimental Investigation using Mössbauer Spectroscopy. American Mineralogist, 95, 545–555.

Carroll, M.R., and Webster, J.D. (1994) Solubilities of sulfur, noble gases, nitrogen, chlorine, and fluorine in magmas. In M.R. Carroll and J.R. Holloway, Eds., Volatiles in Magmas, 30, 231–279. Reviews in Mineralogy, Mineralogical Society of America, Washington, D.C

Dingwell, D.B., and Hess, K-U. (1998) Melt viscosities in the system Na–Fe–Si–O–F–Cl: contrasting effects of F and Cl in alkaline melts American Mineralogist, 83 1016–1021

Evans, K.A., Mavrogenes, J.A., O'Neill, H., Keller, N.S., and Jang, L.Y. (2008) A preliminary investigation of chlorine XANES in silicate glasses. Geochemistry Geophysics and Geosystems, Vol. 9, No. 10

Filiberto, J., and Treiman, A.H. (2009) The effect of chlorine on the liquidus of basalt: First results and implications for basalt genesis on Mars and Earth. Chemical Geology, 263, 60-68.

Filiberto, J., Dasgupta, R., Gross, J., and Treiman, A. (2014) Effect of chlorine on near-liquidus phase equilibria of an Fe–Mg-rich tholeiitic basalt. Contributions to Mineralogy and Petrology, 168, 1-13.

Gaillard, F., Scaillet, B., Pichavant, M., and Bény, J.-M. (2001) The effect of water and fO2 on the ferric-ferrous ratio of silicic melts. Chemical Geology, 174, 255-273.

Jayasuriya, K.D., O'Neill, H.St. C., Berry, A., and Campbell, S.J. (2004) A Mössbauer study of the oxidation state of Fe in silicate melts. American Mineralogist, 89, 1597–1609.

Jenner, F.E., O'Neill, H. St. C., Arculus, R.J., and Mavrogenes, J.A. (2010) The magnetite crisis in the evolution of arc-related magmas and the initial concentration of Au, Ag and Cu. Journal of Petrology, 51, 2445–2464.

Killinc, A., Carmichael, I.S.E, Rivers, M.L., and Sack, R.O. (1983) The ferric ferrous ratio of natural silicate liquids equilibrated in air. Contributions to Mineralogy and Petrology, 83, 136-140.

Kress, V.C., and Carmichael, I.S.E. (1991) The compressibility of silicate liquids containing Fe_2O_3 and the effect of composition, temperature, oxygen fugacity and pressure on their redox states. Contributions to Mineralogy and Petrology, 108, 82-92.

Moore, G., Righter, K., and Carmichael, I.S.E. (1995) The effect of dissolved water on the oxidation state of iron in natural silicate liquids. Contributions to Mineralogy and Petrology, 120, 170–179.

Moore, G., Vennemann, T., and Carmichael, I.S.E. (1998) An empirical model for the solubility of H_2O in magmas to 3 kilobars. American Mineralogist, 83, 36-42.

Moretti, R. (2005) Polymerisation, basicity, oxidation state and their role in ionic modelling of silicate melts. Annals of Geophysics, 48, 583–608.

Mysen, B., Seifert, F., and Virgo, D. (1980) Structure and redox equilibria of iron bearing silicate melts. American Mineralogist, 65, 867–884.

Ottonello, G., Moretti, R., Marini, L., and Vetuschi Zuccolini, M. (2001) Oxidation state of iron in silicate glasses and melts: a thermochemical model. Chemical Geology, 174, 157-179.

Robie R. A., Hemingway B. S., (1995) Thermodynamic Properties of Minerals and Related Substances at 298.15 K and 1 Bar (105 Pascals) Pressure and at Higher Temperatures. U. S. Geological Survey Bulletin, No. 2131, 461pp.

Sack, R.O., Carmichael, I.S.E, Rivers, M.L., and Ghiorso, M.L. (1980) Ferric-ferrous equilibria in natural silicate liquids at 1 bar. Contributions to Mineralogy and Petrology, 75, 369-376

Tangeman, J.A., Lange, R.A., and Forman, L. (2001) Ferric-ferrous equilibria in K_2O-FeO- Fe_2O_3-SiO_2 melts. Geochimica et Cosmochimica Acta, 65, 1809-1819.

Taylor, J.R., Wall, V.J., and Pownceby, M.I. (1992) The calibration and application of accurate redox sensors. American Mineralogist, 77, 284 –295.

Wallace, P.J. (2005) Volatiles in subduction zone magmas: concentrations and fluxes based on melt inclusion and volcanic gas data. Journal of Volcanology and Geothermal Research, 140, 217–240.

Webb, S.L., Bramley, M.J., and Wheeler, A.J. (2014) Rheology and the Fe3+–chlorine reaction in basaltic melts. Chemical Geology, 366, 24-31.

Webster, J.D., and De Vivo, B. (2002) Experimental and modeled solubilities of chlorine in aluminosilicate melts, consequences of magma evolution, and implications for exsolution of hydrous chloride melt at Mt. Somma-Vesuvius. American Mineralogist 87, 1046–1061.

Webster, J.D., Vetere F, Botcharnikov, R.E., Goldoff, B., McBirney A., and Doherty, A.L. (2015) Experimental and modeled chlorine solubilities in aluminosilicate melts at 1 to 7000 bars and 700 to 1250°C: Applications to magmas of Augustine Volcano, Alaska. American Mineralogist In Press.

Wilke, M. (2005) Fe in magma: an overview. Annals of Geophysics, 48, 609-617.

Wilke, M., Behrens H., Burkhard, D.J.M., and Rossano, S. (2002) The oxidation state of iron in silicic melt at 500 MPa water pressure. Chemical Geology, 189, 55.67.

Zimova, M., and Webb, S., 2006. The effect of chlorine on the viscosity of Na_2O–Fe_2O_3–Al_2O_3–SiO_2 melts. American Mineralogist, 91, 344–352.

Table 1

MagLiq Series	T °C	Pressure (MPa)	Duration (Hours)	pH2 (bar)	log fO_2	wt % Cl	wt % FeO[†]	Fe^{3+}/Fe total
MagLiq 5	950	150	333	2.56	-10.1	0.5	4.9 ± 0.13	ND
MagLiq6	950	150	333	2.56	-10.1	0.0	4.2 ± 0.18	ND
MagLiq7	950	130	214	0.86	-9.2	1.0	4.4 ± 0.19	ND
MagLiq8	950	130	214	0.86	-9.2	0.0	3.5 ± 0.13	ND
MagLiq Failed*	950	200	288	2.58	-9.0	0.6 -0.75	3.4 - 5.2	ND
SRD2 Series								
SRD2-2	950	130	138	6.41	-11	0.80	1.0 ± 0.07	0.33
SRD2-4	950	130	132	2.19	-10.1	0.80	1.3 ± 0.15	0.38
SRD2-9	950	130	214	0.85	-9.2	0.70	1.1 ± 0.15	0.42
SRD2-10	950	130	165	22.1	-11.9	0.70	0.6 ± 0.03	0.28

[†]The EPMA determined Fe contents of both the MagLiq series glasses and the SRD glasses are reported by convention as wt% "FeO". The locations of the EPMA analytical spots used to determine the Fe and Cl concentrations in these experiments were distributed randomly throughout the melt volume of the experimental charge from portion of the melt directly adjacent to the magnetite, to the distal portions of the melt at the opposite end of the charge. The values listed in the table are the mean of 15-20 spot analyses; the ± values following the mean are the 1σ standard deviation for the population of EPM analyses.

*The values reported for the MagLiq Failed experiment are the ranges of Cl and Fe contents that were observed in the EPMA transect across the melt of the experimental charge. The approximate location of the analytical transect that produced these values is shown in Fig. 1a.

ND = not determined

Figure 1a and 1b

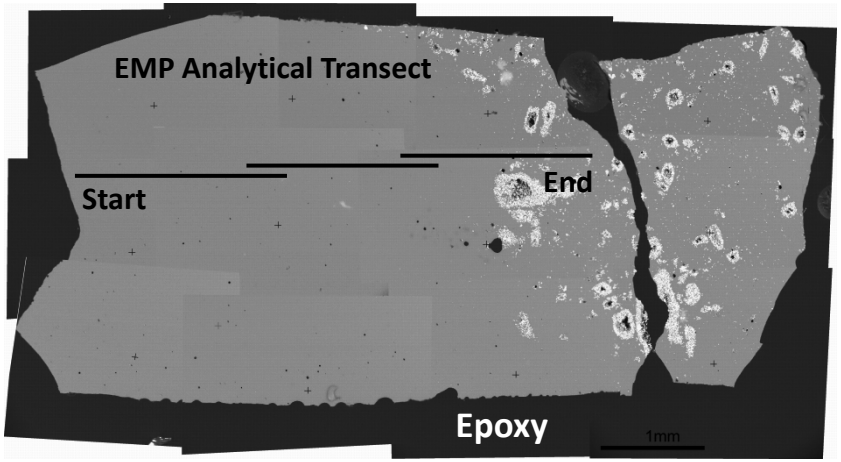

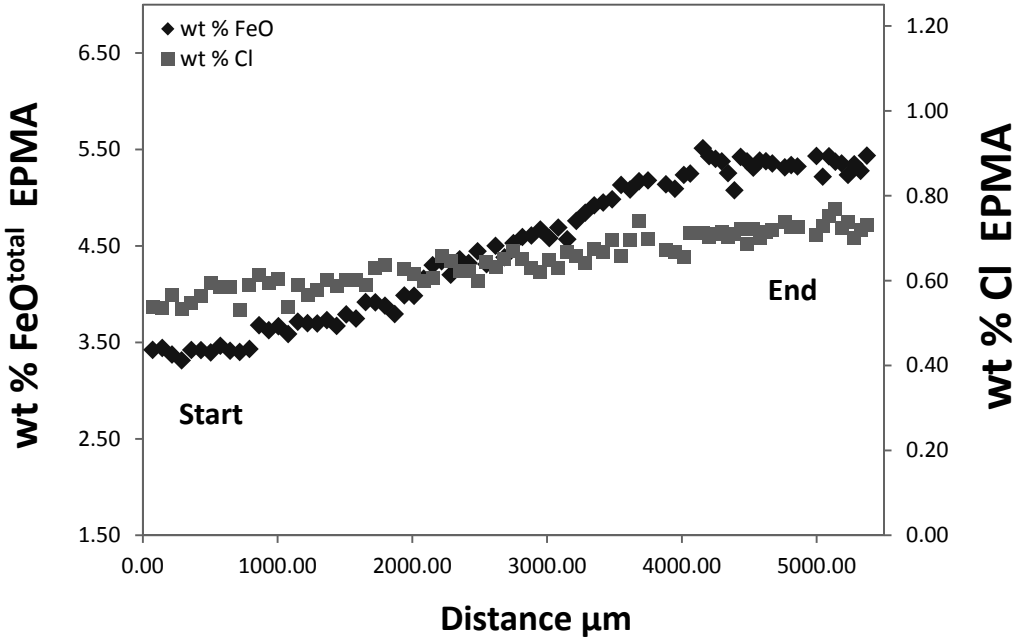

Figure 1. The image in Figure 1a schematically shows the location of the EPMA analytical transect from the MagLiq Failed experiment (see Table 1). The experimental charge shown in the BSE image is comprised of two phases, glass (the light grey phase) and magnetite powder (the bright white phase). Figure 1b shows a plot of FeO and Cl concentrations measured along the length of the transect that is shown in Figure 1a. Distance 0.00 on the x-axis of the plot corresponds to the point labeled “Start” on the BSE image.

Figure 2

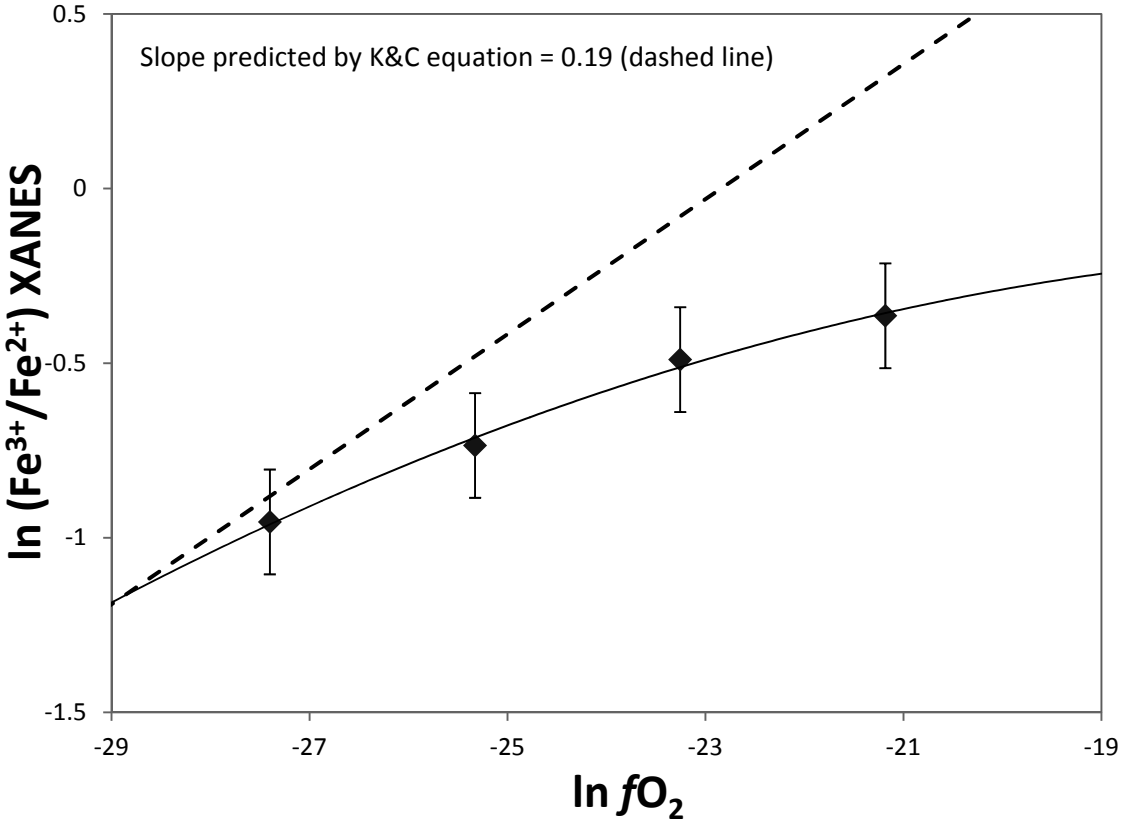

Figure 2 is a ln-ln plot of the XANES measured Fe^{3+}/Fe^{2+} ratios of the SRD Series experiments vs. the experimental fO_2 values. The dashed line represents the slope of the homogenous ferric-ferrous equilibrium as predicted by the Kress and Carmichael equation (1991) which is shown as a frame of reference. The deviation from the predicted slope systematically becomes larger as fO_2 increases.